Possible restoration of particle-hole symmetry in the 5/2-quantized Hall state at small magnetic field

Loïc Herviou● and Frédéric Mila●

Institute of Physics, Ecole Polytechnique Fédérale de Lausanne (EPFL), CH-1015 Lausanne, Switzerland

Motivated by the experimental observation of a quantized 5/2 thermal conductance at filling $\nu = 5/2$, a result incompatible with both the Pfaffian and the anti-Pfaffian states, we have pushed the expansion of the effective Hamiltonian of the 5/2-quantized Hall state to third order in the parameter $\kappa = E_C/\hbar\omega_c \propto 1/\sqrt{B}$ controlling the Landau-level mixing, where E_C is the Coulomb energy and ω_c is the cyclotron frequency. Exact diagonalizations of this effective Hamiltonian show that the difference in overlap with the Pfaffian state and the anti-Pfaffian state induced at second order is reduced by third-order corrections and disappears around $\kappa = 0.4$, suggesting that these states are much closer in energy at smaller magnetic field than previously anticipated. Furthermore, we show that in this range of κ the finite-size spectrum is typical of a quantum phase transition, with a strong reduction of the energy gap and with level crossings between excited states. These results point to the possibility of a quantum phase transition at smaller magnetic field into a phase with an emergent particle-hole symmetry that would explain the measured 5/2 thermal conductance of the 5/2-quantized Hall state.

I. INTRODUCTION

Following up on Laughlin's pioneering explanation of the 1/3 and 1/5 plateaus [1] in terms of wave functions, the theory of the fractional quantum Hall effect (FQHE) has relied to a large extent on variational wave functions, with considerable success thanks, in particular, to Jain's composite fermion theory [2–5]. It was completed by its extension to the Pfaffian (Pf) state by Moore and Read [6,7], and its particle-hole conjugate, the anti-Pfaffian (APf) state [8,9] in order to explain the plateau observed at filling 5/2 [10,11]. This approach has explained many plateaus and has led to the highly nontrivial prediction that the system is gapless at filling 1/2 [12–14]. It seemed that all states observed in the FQHE could be explained in terms of variational wave functions. The alternative approach in terms of an effective Hamiltonian to describe the degeneracy lifting by Coulomb repulsion in a partially filled Landau level has nevertheless proven to be extremely useful. The variational wave functions were shown to be the ground states of parent Hamiltonians that are truncated versions of the effective model [2,15–18]. Effective Hamiltonians have also played a crucial role in discussing the competition between the Pf and the APf states for the 5/2-quantized Hall state [19], with the conclusion that, to second order in $\kappa = E_C/\hbar\omega_c$, where E_C is the Coulomb energy and $\omega_c \propto B$ is the cyclotron frequency, the APf state is favored when the effect of the empty Landau levels is taken into account [20–27]. It thus came as a big surprise when the quantized thermal conductance was found to be equal to 5/2 in the 5/2 plateau [28–30], a value in contradiction with both the APf (3/2) state and the Pf (7/2) state but consistent with particle-hole symmetry. This restored symmetry would be consistent with the particle-hole Pfaffian (PHPf) state [31,32], another candidate for the 5/2

plateau, but this state is usually believed to be gapless and energetically unfavored [33–36], except in a few field-theoretical works [37,38]. Explanations in terms of domains or of lack of equilibration have been put forward [39–54], but as of today there is no consensus on the resolution of this discrepancy.

In view of the impressive corpus of theory, one may wonder if there is still room for the identification of a particle-hole symmetric ground state that would have been missed so far. Our results point towards such an unlikely conclusion. The starting point of our approach is the observation that the effective model is an expansion in $\kappa \propto 1/\sqrt{B}$, hence a high-field expansion. In experimental conditions, the field is around 4 T, and $\kappa \simeq 1.38$ [11]. This large value raises a natural question: Is κ too large in experiments for the second-order expansion to be justified? The only way to answer that question is to push the expansion to higher order in κ, something that has not been attempted so far.

In this paper, we have pushed this expansion to the next order in κ. Although this simply relies on third-order perturbation theory in the Coulomb repulsion, this turned out to be a rather formidable task that could only be carried out with the help of computer-aided formal calculations. As we shall see, the third order changes the physics qualitatively already around $\kappa \simeq 0.3$–0.5, showing that relying on second-order perturbation theory is definitely not justified for $\kappa \simeq 1.38$. The most remarkable effect is that the lifting of the degeneracy in favor of the APf state is counteracted by the third-order term, and that the degeneracy is restored at $\kappa \simeq 0.4$. Moreover, and maybe more importantly, the excitation spectrum of finite-size systems has all the characteristics of a quantum phase transition which, in view of the apparent restoration of particle-hole symmetry between the Pf and the APf states, might lead to a phase with an emergent particle-hole

symmetry. Let us already emphasize, however, that if there is indeed a quantum phase transition, the physics beyond the phase transition cannot be reached by perturbation theory, and any attempt at discussing it on the basis of a truncated perturbative Hamiltonian, as done previously for the second-order model, is prone to fail. Nonperturbative approaches will have to be employed to study that problem.

The paper is organized as follows. In Sec. II, we explain the main ideas of the algorithm we have used to derive the third-order Hamiltonian. In Sec. III A, we compare the results we have obtained at second order with previous results, and in Sec. III B we present and discuss the central results of this paper obtained at third order. Section IV is devoted to two related models that help assess the validity of our approach: a model that only includes the first two Landau levels (Sec. IV A) and a model that assumes full polarization of the lowest Landau level (Sec. IV B). Finally, the implications for the 5/2 quantum Hall state are discussed in Sec. V. Details about all aspects of this study can be found in Appendixes A–D.

II. DERIVATION OF THE EFFECTIVE HAMILTONIAN

We consider two-dimensional electrons on a square torus in a normal magnetic field and in the presence of Coulomb interaction. Up to a constant, the Hamiltonian can be formulated in a second-quantization formalism as

$$\mathcal{H}_{\text{exact}} = \mathcal{H}_0 + \mathcal{H}_1, \tag{1}$$

$$\mathcal{H}_0 = \hbar\omega_c \sum_l l N_l - gB \sum_\sigma \sigma N_\sigma, \tag{2}$$

$$\mathcal{H}_1 = E_C \sum_{\vec{m},\vec{n},\vec{l},\vec{\sigma}} A_{\vec{m},\vec{n}}^{\vec{l},\vec{\sigma}} c_{m_1,l_{m_1},\sigma_{m_1}}^\dagger c_{m_2,l_{m_2},\sigma_{m_2}}^\dagger c_{n_2,l_{n_2},\sigma_{n_2}} c_{n_1,l_{n_1},\sigma_{n_1}}. \tag{3}$$

ω_c is the cyclotron frequency, $E_C = \frac{e^2}{\varepsilon l_B}$ is the Coulomb energy, l_B is the magnetic length, B is the magnetic field, and g is the electronic magnetic moment. In the rest of this paper, we set both l_B and E_C to 1 for simplicity and generally neglect the Zeeman splitting given its magnitude. $l \in \mathbb{N}$ denotes the Landau level, $\sigma = \pm 1$ denotes its spin flavor, N_l denotes the number of electrons in a given Landau level, and N_σ denotes the number of electrons with spin σ. We also denote by L the total number of Landau levels we consider (the spin degeneracy is not included in the counting). We will show results with up to $L = 11$, although our results depend very little on L as soon as $L \geqslant 3$, i.e., when we take into account the influence of the empty Landau levels. Finally, the operator $c_{m,l,\sigma}^\dagger$ creates an electron in the mth orbital of the lth Landau level with spin σ. On a torus, $m \in [0, N_\phi - 1]$ with N_ϕ being the number of elementary magnetic fluxes through the torus. The interaction coefficient $A_{\vec{m},\vec{n}}^{\vec{l},\vec{\sigma}}$ can be straightforwardly obtained for any translation-invariant interaction as detailed in Appendix B. For a Coulomb-like interaction (central and spin-diagonal), symmetry enforces $m_1 + m_2 = n_1 + n_2 [N_\phi]$ and $\sigma_{m_1} + \sigma_{m_2} = \sigma_{n_1} + \sigma_{n_2}$.

In the rest of this paper, we focus on the physics of the 5/2 filled Landau levels. In a strong magnetic field, the splitting of the Landau levels dominates, and it appears reasonable to project the Hamiltonian on its low-energy sector (depending on the filling). Despite the weak Zeeman effect, numerical simulations seem to indicate that the half-filled Landau level is spin polarized. We therefore introduce P_0, the projector on the subspace where the zeroth Landau level is fully occupied for both spin flavors and where the first Landau level with spin $+1$ is half filled. We project the Hamiltonian $\mathcal{H}_{\text{exact}}$ on this subspace and define

$$H_0 = P_0 \mathcal{H}_0 P_0 = E_0 \quad \text{with} \quad E_0 = (\hbar\omega_c - gB)\frac{N_\phi}{2}, \tag{4}$$

$$H_1 = P_0 \mathcal{H}_1 P_0 = E_C \sum_{\vec{m},\vec{n}} A_{\vec{m},\vec{n}}^{\vec{l},\vec{\sigma}} c_{m_1}^\dagger c_{m_2}^\dagger c_{n_2} c_{n_1} + E_C^{0,1}, \tag{5}$$

with $c_n = c_{n,1,+1}$ and $E_C^{0,1}$ being the static energy due to the presence of the filled Landau levels. Note that this energy constant plays a crucial role in the third-order expansion and cannot be neglected. This projected Hamiltonian with no Landau-level mixing has been extensively studied [15,55–59]. On the square torus, it admits six quasidegenerate ground states in six different translation sectors corresponding to the sixfold topological degeneracy of the Pf or APf state. Unless specified, we show results in the $(\pi, 0)$ sector: Our results are largely independent of this choice. This Hamiltonian is particle-hole symmetric at half filling. Due to this symmetry, it cannot discriminate between the Pf and APf phases. The ground state in a given sector is unique and has equal overlap with both Pf and APf states.

In order to reach the experimentally relevant regime, we compute perturbatively the effect of the presence of the empty and occupied Landau levels using $\kappa = \frac{e^2}{\varepsilon\hbar l_B\omega_c}$ as a small parameter. Following Rezayi [27], who performed a calculation to second order, we compute directly the effective Hamiltonian without attempting to project onto pseudopotentials. The development in pseudopotentials is not convenient on a finite torus due to the periodicity, and the complexity of the higher-body terms rises quickly. The second-order and third-order terms of the degenerate perturbative expansion are given by

$$H_2 = -P_0 \mathcal{H}_1 \mathcal{G}_0 \mathcal{H}_1 P_0,$$

$$H_3 = P_0 \mathcal{H}_1 \mathcal{G}_0 \mathcal{H}_1 \mathcal{G}_0 \mathcal{H}_1 P_0 - \frac{1}{2}\{H_1, P_0 \mathcal{H}_1 \mathcal{G}_0^2 \mathcal{H}_1 P_0\}, \tag{6}$$

where

$$\mathcal{G}_0 = \frac{\text{Id} - P_0}{\mathcal{H}_0 - E_0}. \tag{7}$$

H_2 includes two- and three-body terms as discussed in previous works. H_3 also includes an additional four-body term. The five-body terms generated by $P_0 \mathcal{H}_1 \mathcal{G}_0 \mathcal{H}_1 \mathcal{G}_0 \mathcal{H}_1 P_0$ are exactly canceled by the anticommutator.

We perform the numerical computation of the effective Hamiltonians directly at the operator level. The details of our algorithm can be found in Appendix B. As a quick summary, our computational process consists of four parts: (1) computation of the effective interaction in the Landau basis, (2) derivation of all the Feynman diagrams corresponding to $\mathcal{H}_2$ and $\mathcal{H}_3$, (3) exact summation of all processes corresponding to a given diagram, and (4) computation of the effective many-body Hamiltonian and diagonalization. The latter two steps are the most computationally expensive. The complexity of the third step scales as $O(\max(5! L N_\phi^7, (2L)^4 N_\phi^4))$, depending

on the diagrams considered. The fourth step has the standard exponential complexity of exact diagonalization (ED), but with an additional difficulty: The effective Hamiltonian consists of a sum of 3×10^6 n-body operators. To give a concrete illustration, for $N_\phi = 28$, although the symmetry-resolved Hilbert space is only of dimension $\approx 10^5$, it includes $\approx 1.5 \times 10^7$ operators ($\approx 10^6$ if we take into account translation invariance). Even if we were to discard coefficients below 10^{-6}, we would need to apply 3×10^6 operators to each basis element. Consequently, it is not surprising that the effective Hamiltonians themselves are also very dense (approximately a quarter of the matrix elements are nonzero for $N_\phi = 28$). This density limits the practically achievable sizes significantly: Both the memory cost to store the matrix and the cost of applying it to a state become quickly prohibitive.

III. PERTURBATIVE EXPANSION

A. Second-order expansion

We start with a brief discussion of the second-order expansion of $\mathcal{H}_{\text{exact}}$ as a benchmark of our approach. This computation has been previously done on the sphere [20–23,25–27,60] and on the hexagonal torus [25,27], and we verify that we qualitatively and quantitatively recover known results.

Concretely, we work with the Hamiltonian

$$H^{(2)} = H_1 + \kappa H_2 \tag{8}$$

and compute its ground state. In Figs. 1(a)–1(d), we show the low-energy spectrum of $H^{(2)}$. The color represents the difference in overlaps between the Pf and APf states. More precisely, the color is a measure of

$$|\langle \Psi_{\text{Pf}} | \Psi_{\text{ED}} \rangle_c| - |\langle \Psi_{\text{APf}} | \Psi_{\text{ED}} \rangle_c|, \tag{9}$$

with

$$\begin{pmatrix} \langle \Psi_{\text{Pf}} | \Psi_{\text{ED}} \rangle_c \\ \langle \Psi_{\text{APf}} | \Psi_{\text{ED}} \rangle_c \end{pmatrix} = M^{-1} \begin{pmatrix} \langle \Psi_{\text{Pf}} | \Psi_{\text{ED}} \rangle \\ \langle \Psi_{\text{APf}} | \Psi_{\text{ED}} \rangle \end{pmatrix} \tag{10}$$

and

$$M = \begin{pmatrix} \langle \Psi_{\text{Pf}} | \Psi_{\text{Pf}} \rangle & \langle \Psi_{\text{Pf}} | \Psi_{\text{APf}} \rangle \\ \langle \Psi_{\text{APf}} | \Psi_{\text{Pf}} \rangle & \langle \Psi_{\text{APf}} | \Psi_{\text{APf}} \rangle \end{pmatrix}. \tag{11}$$

In Fig. 1(e), we show the overlap of the corresponding ground state with several reference states. At small κ, for $L \geqslant 3$, the second-order expansion favors the APf state (for $L = 2$, the Pf state is actually favored). At $\kappa \approx 0.8$, the gap closes, and a large number of low-energy states collapse onto the ground state. After a transitory regime, a small gap opens. Its ground state is adiabatically connected to the ground state of H_2^{3b}, the three-body contribution of H_2. A second transition then occurs towards the ground state of H_2 (which is approximately also the ground state of H_2^{2b}).

It is important to note the following. Firstly, the collapse of the energy levels we observe at $\kappa \approx 0.8$ is qualitatively different from the typical second-order phase transitions in finite systems. Instead of a well-defined minimum that decreases with the system size, we observe several crossings or anticrossings in the ground state over a range of κ. Secondly, the two large κ phases correspond to a limit where the perturbation theory dominates and are unphysical. The ground
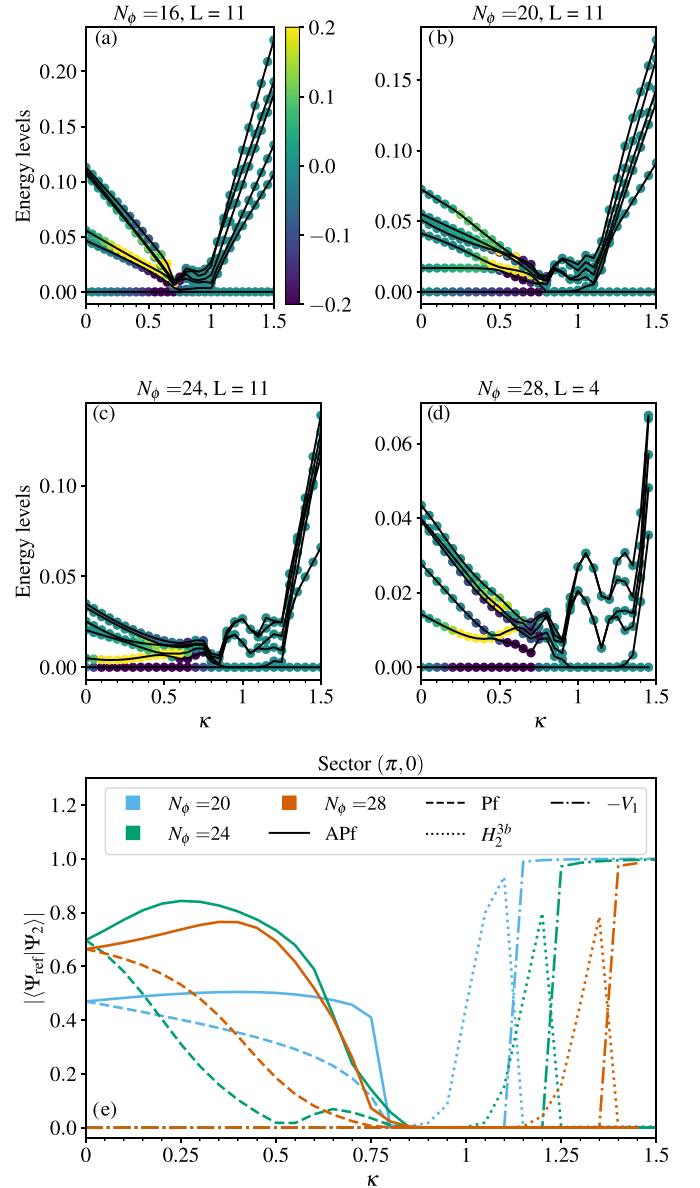

FIG. 1. (a)–(d) Low-energy spectrum in the sector $(\pi, 0)$ at second order. The color code is given in Eq. (9): positive (negative) numbers mark that the Pf (APf) state is favored. (e) Overlap between the ground state and several reference states for different system sizes. Here the overlap is not corrected as in Eq. (9) for simplicity. Below $\kappa \approx 0.8$, the APf state is favored. We then observe a collapse of all low-energy levels. After a small transitional regime, two consecutive phases open. The large $\kappa \geqslant 1.4$ regime is strongly gapped in the translation-invariant sector.

state of H_2^{2b} has nearly perfect overlap with the maximally excited state of the first two-body Haldane pseudopotential V_1. In other words, it is the ground state of a globally attractive potential. Additionally, it becomes $2N_\phi$ degenerate in the limit $\kappa \gg 1$ (in contrast, the topological degeneracy of both the Pf state and the APf state is equal to 6) with ground states in each sector of the form $(\pi, \cdot)$ and $(\cdot, \pi)$. It is particle-hole symmetric, and due to the periodicity of the torus, it is not a simple packed state. The recent results of Ref. [60] could

potentially be explained by a state similar to either of the two large κ phases.

B. Third-order perturbation theory

We now discuss our results for the third-order Hamiltonian

$$H^{(3)} = H_1 + \kappa H_2 + \kappa^2 H_3. \tag{12}$$

We first investigate the effect of $H^{(3)}$ directly on the reference Pf and APf wave functions, before turning to the study of its ground state.

The Pf and APf states have a large overlap with the low-energy eigenstates of the Coulomb Hamiltonian H_1 and are therefore a good first ansatz to qualitatively study the model. If there is an emergent particle-hole symmetry at low energies, they should become degenerate. We therefore investigate the average energy in both states and define the energies per orbital

$$E_{\text{ref}} = \frac{1}{N_\phi} \langle \Psi_{\text{ref}} | H^{(3)} | \Psi_{\text{ref}} \rangle. \tag{13}$$

For $L = 11$, $N_\phi = 24$ in the $(\pi, 0)$ subsector, we obtain

$$E_{\text{Pf}} = -1.3540 - 0.3083\kappa + 0.1015\kappa^2, \tag{14}$$

$$E_{\text{APf}} = -1.3540 - 0.3090\kappa + 0.1033\kappa^2. \tag{15}$$

Due to the particle-hole symmetry, H_1 does not discriminate between these two states, and in agreement with Rezayi [27], H_2 favors the APf state. By contrast, H_3 favors the Pf state. More precisely, its three-body contribution H_3^{3b} favors the Pf state, while the four-body contribution H_3^{4b} still advantages the APf state. For $\kappa_c \approx 0.42$, the Pf state and the APf state are degenerate. We therefore expect a restoration of the particle-hole symmetry in the low-energy subspace near this critical κ. Note that due to finite-size effects, they can have a significant overlap with each other but are orthogonal in the thermodynamic limit. A more complete analysis of the Pf and APf subspace, along with data for different L and N_ϕ, can be found in Appendix C. Our conclusions are unaffected.

We now turn to the study of the ground state of $H^{(3)}$ to confirm this naive approach. In Fig. 2(a), we show the overlaps of the third-order ground state with the Pf state and the APf state, corrected with Eq. (9). While the APf state is still favored at small κ, the amplitude of the difference in overlaps is significantly reduced. For $\kappa \geqslant 0.2$, the difference starts decreasing, and at $\kappa_c \approx 0.4$ the ground state has equal overlap with the Pf and the APf states. κ_c depends very little on the system size, and the ground state becomes particle-hole symmetric as shown in Fig. 3. The low-energy spectrum depicted in Figs. 2(b)–2(e) presents numerous level crossings and a curvature coherent with the finite-size spectrum of a second-order phase transition. Finally, for larger κ, the ground state has a large overlap with the Pf state. All these results are in agreement with the previous naive analysis of Eq. (13). They suggest a possible restoration of the particle-hole symmetry at intermediate κ, which could explain the experimental thermal conductance. In the following section, we discuss the validity of this hypothesis.
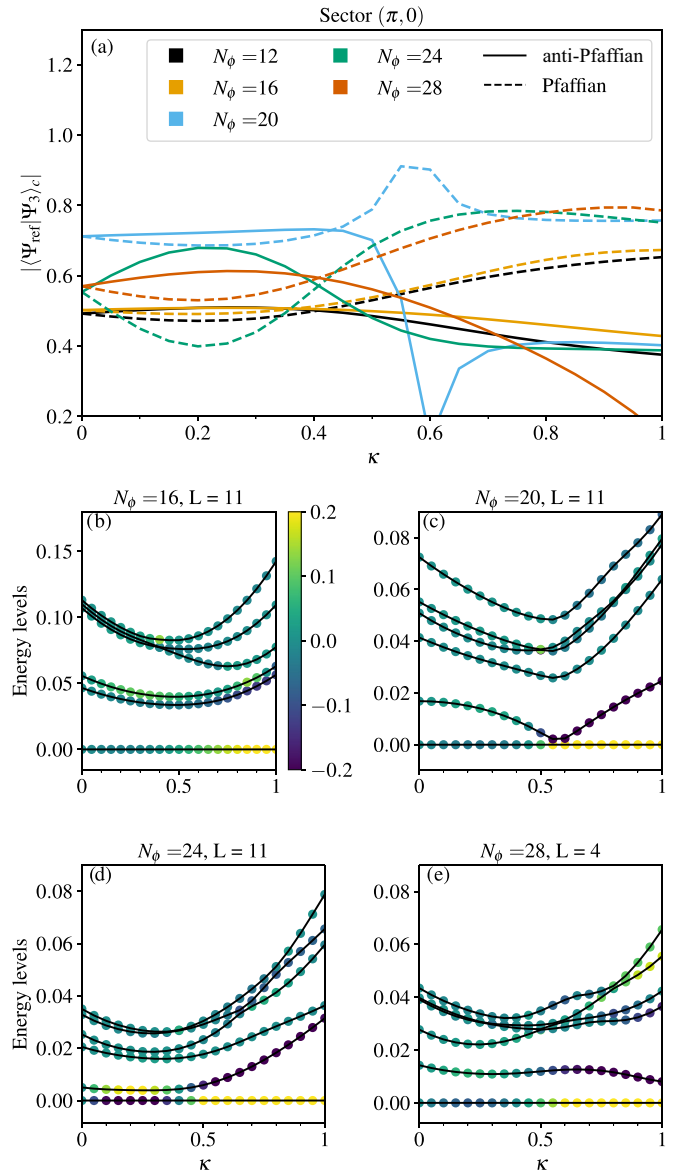

FIG. 2. (a) Overlaps of the third-order ground state with the Pf and APf states. All overlaps are corrected following Eq. (9). (b)–(e) Low-energy spectra. Below $\kappa_c \approx 0.4$, the APf state is favored, while for larger κ, it is the Pf state. We observe a series of energy level crossings strongly reminiscent of a second-order phase transition.

Before that, let us assess the limit of validity of the second-order expansion. In Fig. 4(a), we compare the ground-state energies of $H^{(2)}$ and $H^{(3)}$ for $N_\phi = 28$, and in Fig. 4(b) we measure the overlaps between the two ground states for different values of N_ϕ. The energies already differ at $\kappa = 0.2$ and the overlaps start falling in the range $0.1 \leqslant \kappa \leqslant 0.3$, depending on N_ϕ. The second-order expansion therefore cannot be trusted to describe the experimentally relevant regime.

IV. TWO RELATED MODELS

To put our results in perspective, we discuss in this section two related models: (i) the model $L = 2$ obtained by keeping only the lowest Landau level for the virtual states
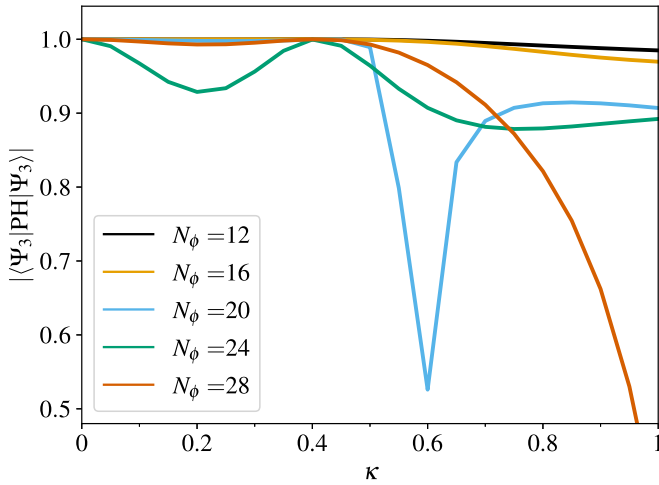
FIG. 3. Overlaps between the third-order ground state and its particle-hole symmetric partner. For all system sizes, the particle-hole symmetry is restored around $\kappa = 0.4$. Note that for most system sizes, it is only weakly broken at low κ.

and (ii) the fully polarized case where all Landau levels are assumed to be filled only by electrons with a given spin polarization. One of the main reasons is that for both models, we can compare the third-order expansion in κ with other approaches, with very encouraging results. Interestingly, the physics of these two models turn out to be significantly different from that of the full model, showing that it is crucial to
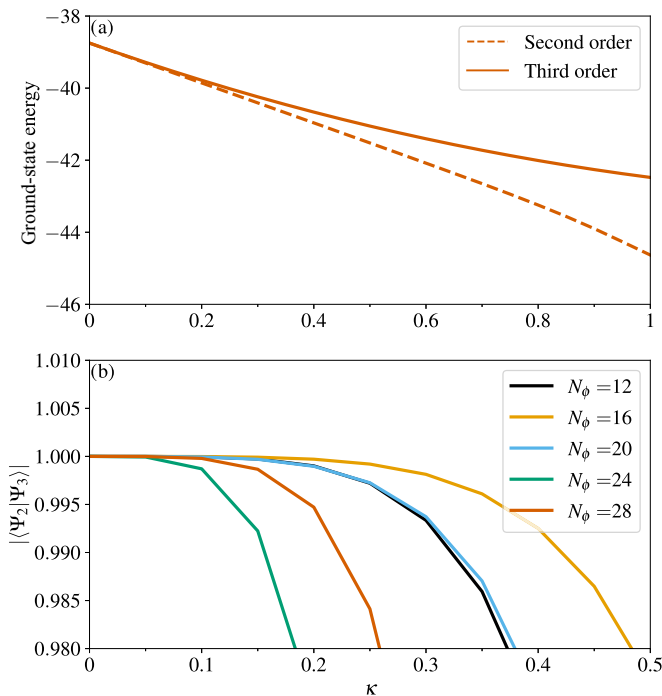

FIG. 4. (a) Ground-state energy for second- and third-order expansion at $N_\phi = 28$ and $L = 3$. Visible differences are already present at $\kappa \approx 0.2$. (b) Overlap between the ground states of $H^{(2)}$ and $H^{(3)}$ at small κ. The expansions agree with an overlap $\geqslant 0.99$ up to $\kappa \approx 0.15$ only.
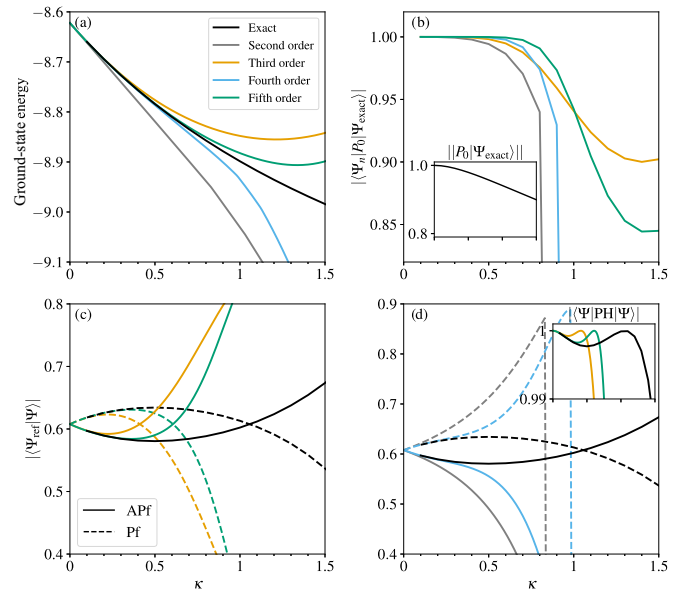

FIG. 5. Comparison between the exact calculation and several orders of the perturbative expansion for spinful electrons with $N_\phi = 8$ and $L = 2$. (a) Ground state of the exact Hamiltonian and the first five orders of the expansion. (b) Overlaps between the perturbative ground states and the normalized projection of the exact ground state. In the inset, we show the norm of the projected ground state. (c) and (d) Comparison of the overlaps with the Pf state and the APf state for odd (c) and even (d) orders. We observe the same overlaps crossing for odd orders as in the exact limit, albeit at much smaller κ. In the inset in (d), overlaps between the ground states and their particle-hole symmetric partners for the exact and odd-order states are shown.

include at least one unoccupied Landau level and to take into account both spin orientations in the lowest Landau level.

A. The $L = 2$ model

The main motivation to investigate this model is that if we keep only the lowest Landau level, we can perform exact diagonalizations and compare the results with a perturbative expansion in κ. The dimension of the Hamiltonian grows as $O\left(N_\phi^{-2} \binom{LN_\phi}{N_{\sigma=+1}} \binom{LN_\phi}{N_{\sigma=-1}}\right)$ after taking into account charge, spin, and momentum conservation and translation invariance. As a consequence, the only nontrivial case on which we could do exact diagonalizations is $N_\phi = 8$ fluxes per Landau level and $L = 2$. Indeed, $N_\phi = 8$ is the smallest system size where one can see a difference between the Pf and APf states, and going to $L = 3$ would mean working with a Hilbert space of dimension 250×10^9 (without taking into account translation invariance, but with charge, spin, and momentum conservation).

We show in Fig. 5(a) the ground-state energy for the exact model and the first five orders of the perturbative expansion. Even for such small systems, we observe a significant deviation of the energy of the second-order correction already at $\kappa \approx 0.2$. Third-order perturbation extends this range of validity up to $\kappa \approx 0.35$. The fifth order is only valid up to $\kappa \approx 0.65$.

In Fig. 5(b), we show the evolution of the overlaps between the perturbative ground states and the projection of the exact

ground state on the spin-polarized manifold. The norm of the projection is represented in the inset. If one stops at an even order, the overlap with the exact ground state falls dramatically as soon as finite-order effects appear. By contrast, the overlap remains significant if one stops at an odd order. The difference comes from the fact that the last term of the expansion is attractive if it is even, and this is not representative of the exact model at large κ. So, to discuss the physics beyond the small-κ range on the basis of a truncated expansion, it is better to stop at an odd order.

More importantly, in Figs. 5(c) and 5(d), we show the overlap of the different ground states with the Pf and APf states. The degeneracy is indeed lifted between the Pf state and the APf state, but if one keeps only the lowest Landau level, it is the Pfaffian state that is favored. So keeping higher Landau levels when including Landau-level mixing is crucial to get the right physics at small κ. At larger κ, the difference in overlap between the Pf state and the APf state decreases, and at $\kappa \approx 1.1$, the ground state of the exact Hamiltonian has a restored particle-hole symmetry, as shown in the inset in Fig. 5(d). Now, as could be anticipated from their poor overlap, even-order ground states systematically miss the emerging particle-hole symmetry. By contrast, the odd-order ground states, and, in particular, the third-order one, agree qualitatively with the restoration of particle-hole symmetry and only underestimate the critical κ_c.

To summarize, the third-order perturbation theory is in qualitative agreement with the exact result on a small cluster regarding the restoration of particle-hole symmetry, but to include more than the fully occupied Landau level when taking into account Landau-level mixing is necessary to get the correct behavior at small κ, namely, the lifting of the degeneracy in favor of the APf state.

B. Fully polarized case

In Ref. [26], Zaletel *et al.* have investigated the ground state of the $\nu = 5/2$ FQHE on an infinite cylinder of finite (but large) circumference using the infinite density matrix renormalization group (iDMRG) algorithm, a method that *exactly* treats Landau-level mixing. In this investigation, the authors of Ref. [26] make two approximations: They only take into account a small number of Landau levels, and they consider spinless electrons, i.e., they assume full polarization, disregarding completely the filled zeroth Landau level of opposite polarization. Up to $\kappa = 1.37$, they found that the APf state is systematically favored, with no sign of a restoration of the particle-hole symmetry.

To compare our perturbative approach with these results, we have performed an investigation of the fully polarized model up to third order in κ. Our results do not show any qualitative differences in the ground-state properties between $L = 4$ and $L = 11$, even if the energies vary significantly, and so keeping only a few Landau levels, as done in Ref. [26], appears to be innocuous. This is not the case for the assumption of full polarization, however. In H_2 (H_3), the down spins do not contribute to the term with the three-body (four-body) operators due to spin conservation and diagrammatic substraction. At second order, only H_2^{3b} distinguishes between the Pf and APf states, and going from spinless to spinful does not
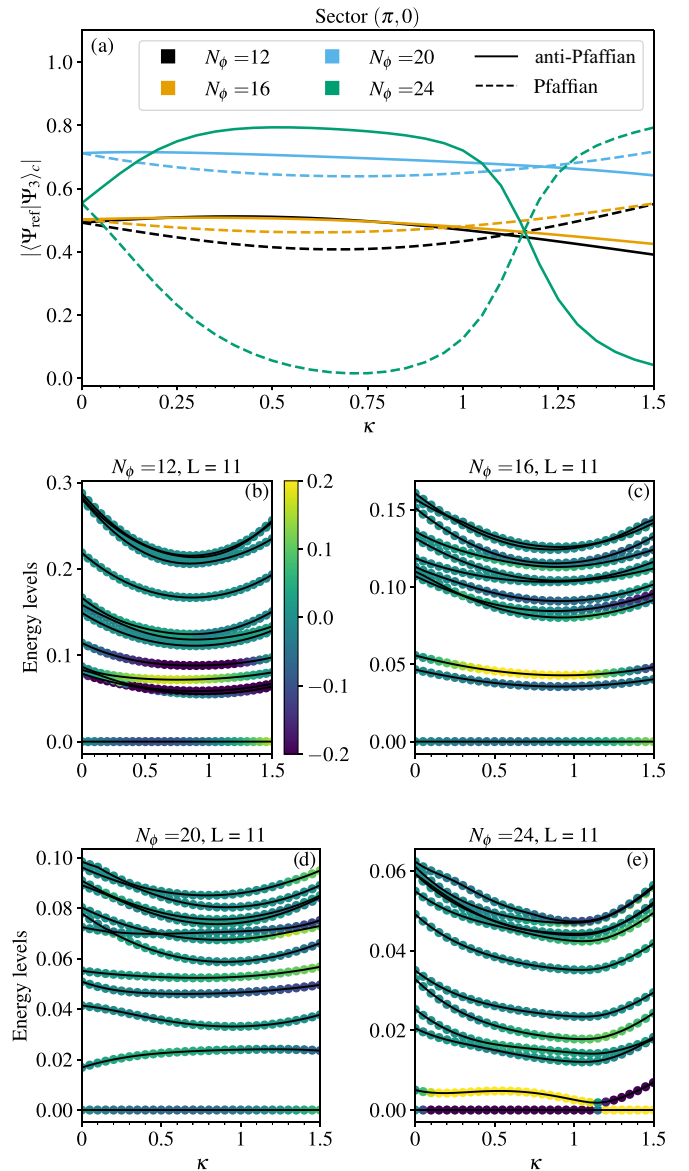

FIG. 6. (a) Overlaps of the third-order ground state for spinless electrons with the Pf and APf states. All overlaps are corrected following Eq. (9). (b)–(e) Corresponding low-energy spectra. While the results are qualitatively similar to the spinful case, the critical $\kappa_c \approx 1$ is well beyond the range of the perturbation theory, and the energy spectra have fewer features.

change the small-κ qualitative result. At third order, this is no longer the case. The down spins do not change H_3^{4b}, but they contribute to H_3^{3b}, and the energy difference induced by this term is reduced for spinless electrons. As a result, the sum of these two contributions, H_3, still favors the Pf state, but with a significantly weaker energy difference. Therefore the APf regime should survive to larger κ.

In order to check this simple argument, we performed both an exact calculation similar to the computation of Sec. IV A for smaller systems, and a third-order expansion at large N_ϕ. The results of the perturbative expansion are presented in Fig. 6. Overlaps with the Pf state and the APf state in Fig. 6(a) show a restoration of the particle-hole symmetry at
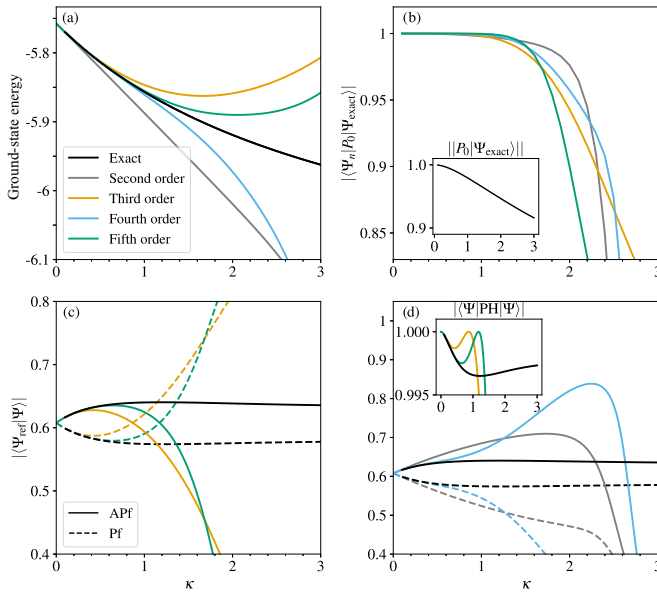
FIG. 7. (a) Energy of the exact ground state for spinless electrons with $L = 2$ and $N_\phi = 8$, compared with the energy obtained from the perturbation theory up to fifth order. (b) Overlaps between the perturbative ground states and the normalized projection of the exact ground state. In the inset, we show the norm of the projected ground state. (c) and (d) Comparison of the overlaps with the Pf state and the APf state for odd (c) and even (d) orders. The particle-hole symmetry is not restored in the exact ground state, in contrast to all the odd-order perturbative expansions. The splitting remains limited as can be seen from the inset in (d) showing the overlaps of the ground state with its particle-hole symmetric partner.

much larger $\kappa_c \simeq 1.1$, well beyond the range of perturbation theory. We also evaluated the effective Hamiltonian in the Pf-APf subspace as well as their average energies. They also predict a critical κ of order 1 (see Appendix C for details). In order to properly interpret these results, it is important to note that, independent of the exact large-κ physics, as long as H_3 opposes H_2, we will always observe a crossing of the overlaps at large κ at third order. So this result should not be interpreted as evidence that a crossing takes place at a much larger κ_c. The fact that the crossing occurs for a very large value of κ could simply indicate the absence of a restoration of the particle-hole symmetry. The quasisaturation of the overlaps with the APf state for $N_\phi = 24$ and $0.35 \leqslant \kappa \leqslant 0.8$ is also strongly reminiscent of the saturation observed in Fig. 7 and a marked difference from what we observed in the spinful limit.

We also note that the excitation spectrum shown in Figs. 6(b)–6(e) has significantly fewer features than in the spinful case, with no obvious tendency to a gap closing, but only an avoided crossing between the two low-lying states for $N_\phi = 24$. These results do not suggest the existence of a phase transition in this region.

The exact calculation presented in Fig. 7 confirms this picture. We computed the ground state of $\mathcal{H}_{exact}$ for spinless electrons with $L = 3$ and $N_\phi = 8$ and $N_\phi = 12$. We only show the results for $N_\phi = 8$ here for comparison with Sec. IV A. Remarkably enough, there is no restoration of the particle-hole symmetry for the exact ground state. As expected, all

expansions stopping at an odd order predict a crossing in overlaps at sufficiently large κ, a clear artifact of truncating the perturbation theory. The odd orders capture the curvature of the overlaps but overcorrect, which should be expected given that the quasisaturation we observe can only be visible in the perturbative expansion if the exact ground state at large κ is also the ground state of the higher-order term of the series. Note that the even orders still predict incorrectly the large-κ limit and severely overestimate the splitting between the Pf state and the APf state.

Altogether, these results point to the possibility of a significant difference between the fully polarized case studied in Ref. [26] and the case where both spin orientations are allowed for in the lowest Landau level.

V. IMPLICATIONS FOR THE 5/2 QUANTUM HALL STATE

Our numerical results demonstrate unambiguously that to third order in κ, and when the spin of the electrons is taken into account, the particle-hole symmetry is restored in the ground state at $\kappa \simeq 0.4$ regardless of the size of the system. What are the physical implications of this result for the actual system? The answer is by necessity speculative because we do not have access to higher orders, but two possibilities emerge which could both, to a certain extent, explain the experimental result of the 5/2 thermal conductivity.

The first possibility is that the Pf state and the APf state remain well separated from the other states, and that the physics is simply controlled by their competition. The fact that they cross at a fairly small value $\kappa = 0.4$ at third order suggests that they will cross at least once even if higher orders are included. This is at the least the case for the $L = 2$ model. This crossing would correspond to a first-order phase transition from the APf state to the Pf state. At the crossing point, the particle-hole symmetry is restored. In the vicinity of this crossing, the ground state will be almost degenerate. If the temperature of the sample is comparable to the level separation, the explanation of Refs. [39,42] in terms of Pf and APf domains due to disorder would be viable if the experimental value $\kappa = 1.38$ is close to this level crossing, or to another one if there are several crossings [61–63] as a function of κ [64].

The second possibility is that the gap to other excitations closes upon increasing κ, and that a (second-order) quantum phase transition occurs at a certain κ_c. The state at $\kappa > \kappa_c$ could simply be the Pf state. However, since the particle-hole symmetry is restored at the transition, the state could also belong to a phase with an emergent particle-hole symmetry. Quite interestingly, this particle-hole symmetric phase would provide a direct explanation for the experimentally measured 5/2-quantized thermal conductance. The existence of a second-order transition is supported by the fact that the excited states come down around the point where particle-hole symmetry is restored at third order before going up again at larger κ. This is typical of the finite-size spectrum of quantum phase transitions as a precursor of criticality in the thermodynamic limit. Note that, since the particle-hole symmetry is broken as soon as $\kappa \neq 0$, the symmetry on the other side of the quantum phase transition has to be an emergent one, i.e., the low-energy physics is that of a particle-hole symmetric

model, but the full spectrum still has traces of the explicit breaking of the particle-hole symmetry in the Hamiltonian. If this possibility is realized, it is important to keep in mind that any finite-order calculation, and, in particular, the third-order one reported here, has nothing to say about the nature of the phase beyond the quantum phase transition. Indeed, at the quantum phase transition, the energy must be singular, implying that the perturbation in κ diverges at that point, or in other words that the expansion in κ of the energy has a finite radius of convergence equal to κ_c. So the fact that the Pf is clearly favored for large κ must be considered as an artifact of the third-order expansion since, for large κ, the ground state must be that of the higher-order term of the series. If the expansion was pushed to higher order, another term would be selected, leading to the stabilization of another state.

In that respect, we would like to note that the first terms of the series contain a hint that the radius of convergence is finite and hence that there is a quantum phase transition. Indeed, as discussed decades ago in the context of high-temperature expansions of thermal phase transitions [65], the radius of convergence is the infinite-order limit of the ratio of subsequent coefficients of the series. The evolution of this ratio with the order can give a hint of the radius of convergence, even if only the first orders are available. In particular, if the ratio decreases with the order, this is a strong indication that the radius of convergence is finite and hence that there is a phase transition. This is illustrated in Appendix D in the case of the one-dimensional (1D) transverse field Ising model, for which we show that the ratio decreases smoothly with the order and that the critical field $h_c = 1$ can be accurately deduced from the first three terms of the series by a polynomial fit. In the present case, the ratio also *decreases* with the order, a behavior consistent with a finite radius of convergence (see Appendix D for details). Given the finite order of the series, let us emphasize that this is just an indication and by no means a proof since the argument relies on the assumption that this ratio is monotonous, an assumption that can only be tested by calculating higher orders.

To summarize, we believe that our results unambiguously point to a change of behavior at small field that could explain the puzzling experimental result of a 5/2 thermal conductance. This is of course not the end of the story, however, because the physics at large κ is *not* accessible to perturbation theory in κ. To finish, let us briefly discuss the alternative approaches that could possibly shed light on the nature of this state.

Since the expansion in κ cannot access this phase, one might be tempted to turn to an expansion in $1/\kappa$, starting from small magnetic field. Unfortunately, this is probably not going to work either. At zero magnetic field, the ground state of the 2D interacting electron gas is a Wigner crystal, and there is almost certainly a phase transition between that state and the 5/2 quantum Hall state we are after. So this state is probably in an intermediate parameter range that cannot be accessed by perturbation theory from either side.

Turning to variational approaches using wave functions is also tricky because the wave functions one can write down explicitly are projected onto a Landau level, and as argued

above we do not have access to an accurate effective model in the range of κ relevant to experiments.

So it seems that the most promising alternative is to turn to numerics to investigate the intermediate-κ regime. This has already been done using DMRG on cylinders for $\nu = 5/2$, but for fully polarized electrons [26], a case for which the physics at third order is clearly different from the spinful case, as explained in Sec. IV B. One obvious suggestion is thus to extend this DMRG calculation to the spinful case.

Finally, we note that tensor network approaches have been successfully developed for 2D models of quantum many-body physics. It would be very interesting to see if these methods can be extended to the FQHE.

APPENDIX A: CONVENTIONS

We work with the following form for the Landau-level orbitals on the torus:

$$
\Psi_{m,l}(x, y) = \frac{1}{\sqrt{L_y \sqrt{\pi} 2^l l!}} \sum_{k=-\infty}^{\infty} e^{\frac{2i\pi}{L_y} y(m+kN_\phi)}
$$
$$
\times H_l\left(x - \frac{2\pi}{L_y}(m+kN_\phi)\right) e^{-(x-\frac{2\pi}{L_y}(m+kN_\phi))^2/2}.
$$
(A1)

We have fixed the gauge such that $\vec{A} = (0, -Bx, 0)$. Here, we denote by L_x (L_y) the dimension of the torus in x (y). In the main text, we consider a square torus with $L_x = L_y = \sqrt{2\pi N_\phi}$. We checked that this does not affect our result. We fixed the magnetic length l_B to 1 for convenience.

APPENDIX B: ALGORITHM

As discussed in the main text, we directly compute the second- and third-order contributions of the empty and occupied Landau levels by using a Schrieffer-Wolff or resolvant type expansion.

The expansion is performed entirely numerically, directly at the operator level in a second-quantization formulation. It can be divided into several conceptually simple steps which can be easily parallelized: (1) computation of the second-quantization coefficients of our chosen interaction for arbitrary Landau levels, (2) generation of all possible Feynman diagrams, (3) computation of the effective coefficients, taking into account normal ordering, and (4)

Evaluation of the matrices and determination of their ground states. In the following, we will briefly summarize some of the key points and difficulties of each step.

1. Interaction coefficients

The computation of second-quantization coefficients is a standard exercise and requires the evaluation of

$$\left\langle \Psi_{m_1,l_{m_1}} \Psi_{m_2,l_{m_2}} \middle| V_C \middle| \Psi_{n_1,l_{n_1}} \Psi_{n_2,l_{n_2}} \right\rangle \tag{B1}$$

for all combinations of m's and l's. The main technical challenge here is the number of such coefficients: $O(N_L^4 N_\phi^3)$. Translation invariance on the torus allows us to compute only $O(N_L^4 N_\phi^2)$ such terms in practice. Naively, each coefficient requires a double integration over $\mathbb{R}^2$, which becomes quickly untractable. Instead, the common approach is to express the interaction in Fourier space

$$V_C = \sum_{\vec{q}} V_C(\vec{q}) e^{i\vec{q}\cdot(\vec{r}_1 - \vec{r}_2)} \tag{B2}$$

and factorize the computation

$$\left\langle \Psi_{m_1,l_{m_1}} \Psi_{m_2,l_{m_2}} \middle| V_C \middle| \Psi_{n_1,l_{n_1}} \Psi_{n_2,l_{n_2}} \right\rangle$$
$$= \sum_{\vec{q}} V_C(\vec{q}) \left\langle \Psi_{m_1,l_{m_1}} \middle| e^{i\vec{q}\cdot\vec{r}} \middle| \Psi_{n_1,l_{n_1}} \right\rangle \left\langle \Psi_{m_2,l_{m_2}} \middle| e^{-i\vec{q}\cdot\vec{r}} \middle| \Psi_{n_2,l_{n_2}} \right\rangle. \tag{B3}$$

Performing the integral on y, after several change of variables we obtain

$$\left\langle \Psi_{m,l_m} \middle| e^{i\vec{q}\cdot\vec{r}} \middle| \Psi_{n,l_n} \right\rangle = \delta'_{m,n+q_y} e^{i\frac{q_x q_y}{2}} e^{i q_x \frac{2\pi}{L_y} n} e^{-\frac{q^2}{4}} \frac{1}{\sqrt{\pi 2^{l_m+l_n} l_m! l_n!}}$$
$$\times \int_{-\infty}^{\infty} H_{l_m}\left(x - \frac{q_y}{2} + i\frac{q_x}{2}\right)$$
$$\times H_{l_n}\left(x + \frac{q_y}{2} + i\frac{q_x}{2}\right) e^{-x^2}. \tag{B4}$$

Note that up to the exponential phase prefactor, this integral no longer depends on m and n. It also decreases exponentially with q^2. We therefore can systematically evaluate it for all values of q_x and q_y up to our precision cutoff, and simply resum the relevant contributions to obtain each of the second-quantization coefficients. In practice, we need of the order of $O(N_\phi^2 L^2)$ such terms for a given precision. The integral can in fact be computed analytically such that

$$\left\langle \Psi_{m,l_m} \middle| e^{i\vec{q}\cdot\vec{r}} \middle| \Psi_{n,l_n} \right\rangle = \delta'_{m,n+q_y} e^{i\frac{q_x q_y}{2}} e^{i q_x \frac{2\pi}{L_y} n} e^{-\frac{q^2}{4}} \frac{1}{\sqrt{\pi 2^{l_m+l_n} l_m! l_n!}}$$
$$\times \sum_{k=0}^{\min l_m, l_n} \binom{l_m}{k} \binom{l_n}{k} 2^k k! (iq_x - q_y)^{l_m-k}$$
$$\times (iq_x + q_y)^{l_n-k}. \tag{B5}$$

We use the above form with heavy memoization in our computation. Finally, we note that it also accepts an interesting formulation in terms of the Lagrange polynomials:

$$\left\langle \Psi_{m,l_m} \middle| e^{i\vec{q}\cdot\vec{r}} \middle| \Psi_{n,l_n} \right\rangle = \delta'_{m,n+q_y} e^{i\frac{q_x q_y}{2}} e^{i q_x \frac{2\pi}{L_y} n} e^{-\frac{q^2}{4}} \begin{cases} L_{l_m}\left(\frac{q^2}{2}\right) & \text{if} \quad l_m = l_n \\ (q_y - iq_x)^{l_m-l_n} \frac{\sqrt{2^{l_n} l_n!}}{\sqrt{2^{l_m} l_m!}} L_{l_m}^{(l_m-l_n)}\left(\frac{q^2}{2}\right) & \text{if} \quad l_m > l_n \\ (q_y + iq_x)^{l_n-l_m} \frac{\sqrt{2^{l_m} l_m!}}{\sqrt{2^{l_n} l_n!}} L_{l_n}^{(l_n-l_m)}\left(\frac{q^2}{2}\right) & \text{if} \quad l_m < l_n. \end{cases} \tag{B6}$$

2. Feynman diagrams

The second- and third-order expansions of the Hamiltonian are given in Eq. (6) in the main text. Terms of the form $P_0 \mathcal{H}_1 \mathcal{G}_0^{m_1} \cdots \mathcal{H}_1 P_0$ can be naturally expressed using Feynman diagrams. While we only compute the perturbation up to third order, we actually have to take into account a large number of diagrams due to the complexity of $\mathcal{H}_1$. It is convenient to separate the Landau levels into three groups: the fully occupied levels, the fully empty ones, and our target. Each operator c or $c^\dagger$ then belongs to three possible groups. For convenience, we strictly order the c ($c^\dagger$) by the label of their Landau levels (and by spin in case of equality). $\mathcal{H}_1$ is then separated into 36 terms, each corresponding to a possible vertex in the Feynman representation of the perturbative expansion. At second order, it is still possible to implement by hand the relevant diagrams: 27 diagrams to obtain all contributions, and only 12 for the nondiagonal ones (neglecting all symmetries). At third order, we have to deal with several hundred diagrams (835 diagrams if we want all contributions, and 458 if we are only interested in the nondiagonal contributions) [66], and it is necessary to do that automatically. Straightforward linear programming

with constraints easily lists all the relevant combination of vortices, which we use as inputs for the last block of our code.

Note that we compute Feynman diagrams leading to diagonal terms in our expansion as they are necessary for the computation of the anticommutators appearing in the third-order contributions. Their computational cost is negligible.

3. Effective interactions

Once we have the list of diagrams, we can compute the effective Hamiltonian in second-quantized form. To do so, we automatically generate all possible combinations of Landau levels and orbitals allowed by the vertices. This can again be done using programming under constraints and memoization to speed up and limit redundant evaluations. The number of orbitals in a given diagram scales approximately as $O(N_\phi^{n_t+n_o/2+n_e/2-3} L_o^{n_o} L_e^{n_e})$, where n_e, n_o, and n_t are the number of operators in empty, occupied, and targeted Landau levels, respectively, and L_e and L_o are the number of empty and occupied Landau levels, respectively. Taking into account the translation invariance allows us to reduce the complexity by an additional factor N_ϕ at the price of symmetrization.

The last step is to normal-order the obtained interactions to keep the number of coefficients to implement manageable. As the complexity is exponential, it is key to implement the normal ordering in a memory-allocation and complexity optimal fashion. The most expensive diagrams to compute are those leading to the five-body terms. They contribute to lower-body terms after normal ordering, even though the five-body interaction itself vanishes as the contribution from $P_0 \mathcal{H}_1 \mathcal{G}_0 \mathcal{H}_1 \mathcal{G}_0 \mathcal{H}_1 P_0$ and the anticommutator exactly cancels.

Parallelization can be realized either at the diagram levels or within the diagrams themselves. We chose the latter for convenience (at the price of a larger memory footprint). For the largest system sizes, it is also more efficient to compute the anticommutator in Eq. (6) directly at the operator levels.

4. Evaluation of the Hamiltonian

Finally, the evaluation of the Hamiltonian from the second-quantization coefficients is straightforward. The main limitation lies in the density of the Hamiltonians which restrict the achievable system sizes. For the largest size considered here $N_\phi = 28$, more than 10×10^6 operators are present in the Hamiltonian if we discard all contributions smaller than 10^{-10} (and 3×10^6 if we choose a cutoff at 10^{-6}). This translates into Hamiltonians that have 25% filling even for $N_\phi = 28$, strongly limiting our possibilities. $N_\phi = 32$, the next relevant size for paired systems (such that the number of electrons remains even), admits $\approx 10^6$ vectors in the translation-invariant basis. Even a 10% filled matrix would occupy approximately 1 TB of RAM (using 64-bit floating points), which is technically achievable but numerically heavy to build and use. Similarly, applying the Hamiltonian on the fly without constructing it would require $\sim 10^{12}$ operations per vector application. While technically achievable, we limited ourselves to $N_\phi = 28$ given the massive numerical costs.

The explosion of the number of coefficients will actually also hard-limit the possible orders of the expansion as long as we keep this second-quantized formulation. Even including only the five-body terms appearing at the next order would require the computation and evaluation of 100×10^6 operators per basis state. Given the results of the exact calculation for small systems (even-order expansions are physically wrong faster than the odd order), it appears impractical or impossible to extend this naive expansion up to fifth order in the foreseeable future. Other approaches such as DMRG would be more appropriate.

APPENDIX C: EFFECTIVE HAMILTONIANS BETWEEN PFAFFIAN AND ANTI-PFAFFIAN STATES

This Appendix summarizes the effective Hamiltonians we obtained in the Pf-APf subspace. They are included in this Appendix both as a reference for benchmarking and to illustrate the opposite effects of the second- and third-order perturbative expansion. Concretely, we define the reduced effective Hamiltonian

$$h_n = \frac{1}{N_{l=1}} \begin{pmatrix} \Psi_{\mathrm{Pf}} & \Psi_{\mathrm{APf}} \end{pmatrix} H_n \begin{pmatrix} \Psi_{\mathrm{Pf}} \\ \Psi_{\mathrm{APf}} \end{pmatrix}. \tag{C1}$$

Due to the nonorthogonality of the states, we also investigate the corrected effective Hamiltonian

$$\tilde{h}_n = M^{-\frac{1}{2}} h_n M^{-\frac{1}{2}} \tag{C2}$$

with M defined in Eq. (9). $\tilde{h}_n$ is in principle a better measure of the energy splitting and the coupling between the Pf and APf states. Our conclusions are nonetheless unaffected.

First, we show the results for the spinful system. In Table I, we directly list the effective Hamiltonian h_n defined in Eq. (C1) in the Pauli matrix basis. In Table II, we present $\tilde{h}_n$ for the same systems. h_n sees more significant finite-size effects, even at fixed L. The crossing point is reliably at $\kappa_c \approx 0.4$. The Padé $(1, 1)$ approximant of the series (h_1, h_2, h_3) gives similar results, with a restoration of the particle-hole symmetry at $\kappa_c \approx 0.6$. In Tables III and IV, we show the same quantities for spinless systems, with $\kappa_c \approx 1$. The influence of the third-order expansion is reduced. If we perform the same Padé $(1, 1)$ approximant, κ_c is pushed above 2 with significant variations with the system size. Note nonetheless that this approximant is here extremely sensitive to the details of the computation: Were we to not include the trivial constant terms in H_3, we would see no crossing for any N_ϕ.

APPENDIX D: PERTURBATIVE EXPANSION AND QUANTUM PHASE TRANSITION

In this Appendix, we discuss in more detail the connection between the perturbative expansion of the ground-state energy of a Hamiltonian as a function of a parameter, say, x, and the occurrence of a quantum phase transition at a critical parameter x_c. In the context of thermal phase transitions, this has been discussed at length [65] for high-temperature expansions. If a phase transition occurs at inverse temperature β_c, this means that the free energy has a singularity, which in turns implies that the radius of convergence of the series must be equal to β_c. By analogy, a quantum phase transition can be expected to take place at x_c if the radius of convergence of the series of the ground-state energy is finite and equal to x_c.

Now, if we denote by a_n the coefficients of the expansion of the ground energy, the radius of convergence is given by the limit of $|a_{n-1}/a_n|$ when n goes to infinity. In principle, this implies that one should know the series to infinite order to know if there is a quantum critical point. However, if the series is well behaved, the first terms of the series can already contain some relevant information. In particular, if the ratio $|a_{n-1}/a_n|$ decreases with n, the radius of convergence cannot be infinite, and a quantum phase transition has to take place.

Let us consider as an example the transverse field Ising model whose Hamiltonian is

$$H = -J \sum_j \sigma_j^x \sigma_{j+1}^x - h \sum_j \sigma_j^z. \tag{D1}$$

The exact expression for the ground-state energy as a function of the transverse field h [67] can be used to evaluate the coefficients of the expansion. All odd coefficients vanish, and the even coefficients are given by $a_0 = -1$ and

$$a_n = -\prod_{p=2,\, p\ \mathrm{even}}^n \left(\frac{p-3}{p} \right)^2, \quad n \geqslant 2. \tag{D2}$$

TABLE I. Effective Hamiltonians in the Pf-APf subspace for spinful electrons, defined in Eq. (C1). We use the notation $h_n = n_0 \sigma^0 + n_x \sigma^x + n_z \sigma^z \equiv (n_0, n_z, n_x)$.

N_ϕ	Sector	L	h_1	h_2	h_3
28	$(\pi, 0)$	4	$(-1.3829, 0, -0.2279)$	$(-0.1983, 0.0004, -0.0322)$	$(0.0657, -0.0009, 0.0103)$
28	(π, π)	4	$(-1.3828, 0, -0.6516)$	$(-0.1983, 0.0003, -0.0925)$	$(0.0652, -0.0008, 0.0291)$
24	$(\pi, 0)$	11	$(-1.354, 0, -0.3511)$	$(-0.3087, 0.0004, -0.0796)$	$(0.1024, -0.0009, 0.0256)$
24	(π, π)	11	$(-1.3539, 0, -0.4565)$	$(-0.3087, 0.0004, -0.1038)$	$(0.102, -0.001, 0.0334)$
20	$(\pi, 0)$	11	$(-1.3172, 0, -0.4494)$	$(-0.3084, 0.0003, -0.1049)$	$(0.102, -0.0008, 0.0338)$
20	(π, π)	11	$(-1.3172, 0, -0.118)$	$(-0.3085, 0.0004, -0.0274)$	$(0.1024, -0.0009, 0.0086)$
16	$(\pi, 0)$	11	$(-1.268, 0, -0.658)$	$(-0.308, 0.0003, -0.1581)$	$(0.1024, -0.0008, 0.0514)$
16	(π, π)	11	$(-1.2687, 0, -0.9211)$	$(-0.3074, 0.0003, -0.2207)$	$(0.1029, -0.0007, 0.0725)$
12	$(\pi, 0)$	11	$(-1.1948, 0, -0.9699)$	$(-0.3088, 0.0005, -0.2488)$	$(0.1028, -0.0011, 0.0812)$
12	(π, π)	11	$(-1.1947, 0, -0.4337)$	$(-0.3104, 0.0005, -0.1107)$	$(0.1077, -0.0013, 0.0382)$

TABLE II. Effective Hamiltonians $\tilde{h}_n = M^{-\frac{1}{2}} h_n M^{-\frac{1}{2}}$ in the Pf-APf subspace corrected by the overlap matrix for spinful electrons. We round at the fourth decimal.

N_ϕ	Sector	L	$\tilde{h}$	$\tilde{h}_2$	$\tilde{h}_3$
28	$(\pi, 0)$	4	$(-1.3828, 0, -0.0003)$	$(-0.1984, 0.0004, 0.0005)$	$(0.0658, -0.0009, -0.0005)$
28	(π, π)	4	$(-1.3826, 0, -0.0006)$	$(-0.1988, 0.0004, 0.0011)$	$(0.0661, -0.0009, -0.002)$
24	$(\pi, 0)$	11	$(-1.354, 0, -0.0001)$	$(-0.3088, 0.0004, 0.0004)$	$(0.1027, -0.0009, -0.001)$
24	(π, π)	11	$(-1.3538, 0, -0.0001)$	$(-0.3088, 0.0004, 0.0004)$	$(0.1024, -0.001, -0.0011)$
20	$(\pi, 0)$	11	$(-1.3172, 0, -0.0001)$	$(-0.3085, 0.0004, 0.0004)$	$(0.1024, -0.0008, -0.0012)$
20	(π, π)	11	$(-1.3172, 0, 0)$	$(-0.3085, 0.0004, 0.0002)$	$(0.1025, -0.0009, -0.0006)$
16	$(\pi, 0)$	11	$(-1.2671, 0, -0.0016)$	$(-0.309, 0.0004, 0.002)$	$(0.1036, -0.0009, -0.0023)$
16	(π, π)	11	$(-1.2659, 0, -0.0038)$	$(-0.3107, 0.0004, 0.0045)$	$(0.1059, -0.001, -0.0042)$
12	$(\pi, 0)$	11	$(-1.1921, 0, -0.0033)$	$(-0.3125, 0.0008, 0.0046)$	$(0.1079, -0.0019, -0.0063)$
12	(π, π)	11	$(-1.194, 0.0, -0.0019)$	$(-0.3111, 0.0006, 0.0018)$	$(0.108, -0.0014, -0.0009)$

TABLE III. Effective Hamiltonians in the Pf-APf subspace for spinless electrons, defined in Eq. (C1). We use the notation $h_n = n_0 \sigma^0 + n_x \sigma^x + n_z \sigma^z \equiv (n_0, n_z, n_x)$.

N_ϕ	Sector	L	h_1	h_2	h_3
24	$(\pi, 0)$	11	$(-0.8849, 0, -0.2295)$	$(-0.0289, 0.0004, -0.0071)$	$(0.0067, -0.0003, 0.0015)$
24	(π, π)	11	$(-0.8848, 0, -0.2984)$	$(-0.0287, 0.0004, -0.0092)$	$(0.0066, -0.0003, 0.002)$
20	$(\pi, 0)$	11	$(-0.8629, 0, -0.2944)$	$(-0.0288, 0.0003, -0.0093)$	$(0.0066, -0.0003, 0.002)$
20	(π, π)	11	$(-0.8629, 0, -0.0773)$	$(-0.029, 0.0004, -0.0024)$	$(0.0067, -0.0003, 0.0005)$
16	$(\pi, 0)$	11	$(-0.8335, 0, -0.433)$	$(-0.029, 0.0003, -0.0144)$	$(0.0069, -0.0003, 0.0032)$
16	(π, π)	11	$(-0.8342, 0, -0.6063)$	$(-0.0293, 0.0003, -0.0206)$	$(0.0071, -0.0003, 0.0048)$
12	$(\pi, 0)$	11	$(-0.7892, 0, -0.641)$	$(-0.0286, 0.0005, -0.0224)$	$(0.0068, -0.0004, 0.005)$
12	(π, π)	11	$(-0.7891, 0, -0.287)$	$(-0.0306, 0.0005, -0.0108)$	$(0.0077, -0.0005, 0.0025)$

TABLE IV. Effective Hamiltonians $\tilde{h}_n = M^{-\frac{1}{2}} h_n M^{-\frac{1}{2}}$ in the Pf-APf subspace corrected by the overlap matrix for spinless electrons.

N_ϕ	Sector	L	$\tilde{h}$	$\tilde{h}_2$	$\tilde{h}_3$
24	$(\pi, 0)$	11	$(-0.8849, 0, -0.0001)$	$(-0.0291, 0.0004, 0.0004)$	$(0.0067, -0.0003, -0.0002)$
24	(π, π)	11	$(-0.8848, 0, -0.0001)$	$(-0.0289, 0.0004, 0.0005)$	$(0.0066, -0.0003, -0.0003)$
20	$(\pi, 0)$	11	$(-0.8629, 0, -0.0001)$	$(-0.029, 0.0004, 0.0005)$	$(0.0067, -0.0003, -0.0003)$
20	(π, π)	11	$(-0.8629, 0, 0)$	$(-0.029, 0.0004, 0.0002)$	$(0.0067, -0.0003, -0.0001)$
16	$(\pi, 0)$	11	$(-0.8327, 0, -0.0016)$	$(-0.0294, 0.0004, 0.0008)$	$(0.0071, -0.0003, -0.0005)$
16	(π, π)	11	$(-0.8315, 0, -0.0038)$	$(-0.0303, 0.0004, 0.0014)$	$(0.0076, -0.0004, -0.0008)$
12	$(\pi, 0)$	11	$(-0.7866, 0, -0.0033)$	$(-0.0305, 0.0008, 0.0023)$	$(0.0079, -0.0006, -0.0014)$
12	(π, π)	11	$(-0.7884, 0, -0.0019)$	$(-0.0307, 0.0006, 0.0003)$	$(0.0078, -0.0005, -0.0003)$

TABLE V. Ground-state energy per particle and its first two derivatives estimated from the third-order perturbative expansion for different N_ϕ and L. Higher derivatives cannot be estimated from the expansion. For $N_\phi = 8$, we performed the computation exactly, and we have access to higher orders of the derivative.

N_ϕ	L	$E_3(\pi, 0)$	$\partial_\kappa E_3(\pi, 0)$	$\partial_\kappa^2 E_3(\pi, 0)$	$E_3(\pi, \pi)$	$\partial_\kappa E_3(\pi, \pi)$	$\partial_\kappa^2 E_3(\pi, \pi)$
28	4	−1.3839	−0.1974	0.1316	−1.384	−0.1973	0.1322
24	11	−1.3548	−0.3081	0.2044	−1.3549	−0.3085	0.2063
24	4	−1.3548	−0.1979	0.1316	−1.3549	−0.1982	0.134
20	11	−1.3187	−0.308	0.2087	−1.3181	−0.3082	0.2077
20	4	−1.3187	−0.1976	0.1365	−1.3181	−0.1979	0.1353
16	11	−1.27	−0.3062	0.2045	−1.2704	−0.3059	0.2044
16	4	−1.27	−0.1959	0.1322	−1.2704	−0.1955	0.1323
12	11	−1.1963	−0.3076	0.2055	−1.1959	−0.3093	0.2142
12	4	−1.1963	−0.1973	0.1326	−1.1959	−0.199	0.142
N_ϕ	L	$E(\pi, 0)$	$\partial_\kappa E(\pi, 0)$	$\partial_\kappa^2 E(\pi, 0)$	$\partial_\kappa^3 E(\pi, 0)$	$\partial_\kappa^4 E(\pi, 0)$	
8	2	−1.0778	−0.04912	0.04228	−0.0590	0.115	

For $n \geqslant 4$, $(a_{n-2}/a_n)^{1/2} = \frac{n}{n-3}$. The radius of convergence is thus given by

$$h_c = \lim_{n \to \infty} (a_{n-2}/a_n)^{1/2} = \lim_{n \to \infty} 1 + \frac{3}{n-3} = 1 \quad \text{(D3)}$$

or equivalently by

$$1/h_c = \lim_{n \to \infty} (a_n/a_{n-2})^{1/2} = \lim_{n \to \infty} 1 - \frac{3}{n} = 1. \quad \text{(D4)}$$

The radius of convergence is $h_c = 1$, in agreement with the exact result, but more importantly the ratio $(a_{n-2}/a_n)^{1/2}$ decreases with n for $n \geqslant 4$. Besides, expressed as a function of $1/n$, the ratio giving $1/h_c$, $(a_n/a_{n-2})^{1/2}$, reduces to a polynomial of degree 1. Hence a linear regression of this ratio for the first two terms, $n = 4$ and $n = 6$, gives the correct limit, $h_c = 1$.

For our model, we have computed the derivatives of the ground-state energy for the third-order perturbation Hamiltonian and for the exact Hamiltonian with $L = 2$. They are listed in Table V. In terms of the derivatives, coefficients and their ratio are given by

$$a_n = \frac{1}{n!} \partial_\kappa^n E(\kappa = 0), \quad \text{(D5)}$$

$$a_{n-1}/a_n = n \partial_\kappa^{n-1} E(\kappa = 0)/\partial_\kappa^n E(\kappa = 0). \quad \text{(D6)}$$

For our ground state, the ratio a_{n-1}/a_n also decreases between $n = 1$ and $n = 2$. Taken naively at $n = 2$, it gives $\kappa_c \approx 3$ for $L = 4$ and $L = 10$. These values of course are but naive approximations, and should just be seen as a suggestion of the existence of a critical point. For $L = 2$, we extracted the first four derivatives following our exact computation, and we found $\kappa_c \approx 2$ performing a naive linear regression.

[1] R. B. Laughlin, Phys. Rev. Lett. **50**, 1395 (1983).

[2] F. D. M. Haldane, Phys. Rev. Lett. **51**, 605 (1983).

[3] B. I. Halperin, Phys. Rev. Lett. **52**, 1583 (1984).

[4] J. K. Jain, Phys. Rev. Lett. **63**, 199 (1989).

[5] B. I. Halperin and J. K. Jain, *Fractional Quantum Hall Effects* (World Scientific, Singapore, 2020).

[6] G. Moore and N. Read, Nucl. Phys. B **360**, 362 (1991).

[7] N. Read and G. Moore, Prog. Theor. Phys. Suppl. **107**, 157 (1992).

[8] M. Levin, B. I. Halperin, and B. Rosenow, Phys. Rev. Lett. **99**, 236806 (2007).

[9] S.-S. Lee, S. Ryu, C. Nayak, and M. P. A. Fisher, Phys. Rev. Lett. **99**, 236807 (2007).

[10] R. Willett, J. P. Eisenstein, H. L. Störmer, D. C. Tsui, A. C. Gossard, and J. H. English, Phys. Rev. Lett. **59**, 1776 (1987).

[11] J. S. Xia, W. Pan, C. L. Vicente, E. D. Adams, N. S. Sullivan, H. L. Stormer, D. C. Tsui, L. N. Pfeiffer, K. W. Baldwin, and K. W. West, Phys. Rev. Lett. **93**, 176809 (2004).

[12] B. I. Halperin, P. A. Lee, and N. Read, Phys. Rev. B **47**, 7312 (1993).

[13] R. L. Willett, R. R. Ruel, K. W. West, and L. N. Pfeiffer, Phys. Rev. Lett. **71**, 3846 (1993).

[14] V. W. Scarola, K. Park, and J. K. Jain, Nature (London) **406**, 863 (2000).

[15] M. Greiter, X.-G. Wen, and F. Wilczek, Phys. Rev. Lett. **66**, 3205 (1991).

[16] C. H. Lee, Z. Papić, and R. Thomale, Phys. Rev. X **5**, 041003 (2015).

[17] L. Chen, S. Bandyopadhyay, and A. Seidel, Phys. Rev. B **95**, 195169 (2017).

[18] S. Bandyopadhyay, G. Ortiz, Z. Nussinov, and A. Seidel, Phys. Rev. Lett. **124**, 196803 (2020).

[19] K. K. W. Ma, M. R. Peterson, V. W. Scarola, and K. Yang, arXiv:2208.07908.

[20] A. Wójs, C. Tőke, and J. K. Jain, Phys. Rev. Lett. **105**, 096802 (2010).

[21] E. H. Rezayi and S. H. Simon, Phys. Rev. Lett. **106**, 116801 (2011).

[22] M. R. Peterson and C. Nayak, Phys. Rev. B **87**, 245129 (2013).

[23] S. H. Simon and E. H. Rezayi, Phys. Rev. B **87**, 155426 (2013).

[24] I. Sodemann and A. H. MacDonald, Phys. Rev. B **87**, 245425 (2013).

[25] K. Pakrouski, M. R. Peterson, T. Jolicoeur, V. W. Scarola, C. Nayak, and M. Troyer, Phys. Rev. X **5**, 021004 (2015).

[26] M. P. Zaletel, R. S. Mong, F. Pollmann, and E. H. Rezayi, Phys. Rev. B **91**, 045115 (2015).

[27] E. H. Rezayi, Phys. Rev. Lett. **119**, 026801 (2017).

[28] M. Banerjee, M. Heiblum, V. Umansky, D. E. Feldman, Y. Oreg, and A. Stern, Nature (London) **559**, 205 (2018).

[29] B. Dutta, V. Umansky, M. Banerjee, and M. Heiblum, Science **377**, 1198 (2022).

[30] B. Dutta, W. Yang, R. Melcer, H. K. Kundu, M. Heiblum, V. Umansky, Y. Oreg, A. Stern, and D. Mross, Science **375**, 193 (2022).

[31] T. Jolicoeur, Phys. Rev. Lett. **99**, 036805 (2007).

[32] D. T. Son, Phys. Rev. X **5**, 031027 (2015).

[33] A. C. Balram, M. Barkeshli, and M. S. Rudner, Phys. Rev. B **98**, 035127 (2018).

[34] R. V. Mishmash, D. F. Mross, J. Alicea, and O. I. Motrunich, Phys. Rev. B **98**, 081107(R) (2018).

[35] M. Yutushui and D. F. Mross, Phys. Rev. B **102**, 195153 (2020).

[36] E. H. Rezayi, K. Pakrouski, and F. D. M. Haldane, Phys. Rev. B **104**, L081407 (2021).

[37] L. Antonić, J. Vučičević, and M. V. Milovanović, Phys. Rev. B **98**, 115107 (2018).

[38] S. Đurđević and M. V. Milovanović, Phys. Rev. B **100**, 195303 (2019).

[39] X. Wan and K. Yang, Phys. Rev. B **93**, 201303(R) (2016).

[40] P. T. Zucker and D. E. Feldman, Phys. Rev. Lett. **117**, 096802 (2016).

[41] S. H. Simon, Phys. Rev. B **97**, 121406(R) (2018).

[42] C. Wang, A. Vishwanath, and B. I. Halperin, Phys. Rev. B **98**, 045112 (2018).

[43] D. F. Mross, Y. Oreg, A. Stern, G. Margalit, and M. Heiblum, Phys. Rev. Lett. **121**, 026801 (2018).

[44] B. Lian and J. Wang, Phys. Rev. B **97**, 165124 (2018).

[45] D. E. Feldman, Phys. Rev. B **98**, 167401 (2018).

[46] S. H. Simon, Phys. Rev. B **98**, 167402 (2018).

[47] K. K. W. Ma and D. E. Feldman, Phys. Rev. B **99**, 085309 (2019).

[48] J. Park, C. Spånslätt, Y. Gefen, and A. D. Mirlin, Phys. Rev. Lett. **125**, 157702 (2020).

[49] I. C. Fulga, Y. Oreg, A. D. Mirlin, A. Stern, and D. F. Mross, Phys. Rev. Lett. **125**, 236802 (2020).

[50] S. H. Simon, M. Ippoliti, M. P. Zaletel, and E. H. Rezayi, Phys. Rev. B **101**, 041302(R) (2020).

[51] S. H. Simon and B. Rosenow, Phys. Rev. Lett. **124**, 126801 (2020).

[52] H. Asasi and M. Mulligan, Phys. Rev. B **102**, 205104 (2020).

[53] K. K. W. Ma and D. E. Feldman, Phys. Rev. Lett. **125**, 016801 (2020).

[54] W. Zhu, D. N. Sheng, and K. Yang, Phys. Rev. Lett. **125**, 146802 (2020).

[55] D. Yoshioka, Phys. Rev. B **29**, 6833 (1984).

[56] R. H. Morf, Phys. Rev. Lett. **80**, 1505 (1998).

[57] K. Park, V. Melik-Alaverdian, N. E. Bonesteel, and J. K. Jain, Phys. Rev. B **58**, R10167 (1998).

[58] E. H. Rezayi and F. D. M. Haldane, Phys. Rev. Lett. **84**, 4685 (2000).

[59] A. Wójs, Phys. Rev. B **63**, 125312 (2001).

[60] S. Das, S. Das, and S. S. Mandal, arXiv:2206.04419.

[61] S. Hegde, V. Shivamoggi, S. Vishveshwara, and D. Sen, New J. Phys. **17**, 053036 (2015).

[62] S. S. Hegde and S. Vishveshwara, Phys. Rev. B **94**, 115166 (2016).

[63] G. Vionnet, B. Kumar, and F. Mila, Phys. Rev. B **95**, 174404 (2017).

[64] This is, for instance, what happens to the two low-lying states of the Kitaev chain when the pairing is smaller than the hopping, in which case they cross as a function of the chemical potential a number of times equal to the number of sites provided the calculation is exact or at least carried out in perturbation theory to an order equal to the number of sites.

[65] C. Domb and J. J. L. Lebowitz, *Phase Transitions and Critical Phenomena*, Phase Transitions and Critical Phenomena (Elsevier, Burlington, MA, 2000), Vol. 19.

[66] In practice, this number can be reduced by a factor of 2 by a combination of Hermitian conjugation and anticommutation.

[67] B. K. Chakrabarti, A. Dutta, and P. Sen, *Quantum Ising Phases and Transitions in Transverse Ising Models*, Lecture Notes in Physics (Springer, New York, 1996), Vol. 862.